REPORT DOCUMENTATION PAGE

Form Approved
OMB No. 0704-0188

1. REPORT DATE *(DD-MM-YYYY)*	2. REPORT TYPE	3. DATES COVERED *(From - To)*
	Technical Papers	

4. TITLE AND SUBTITLE

5a. CONTRACT NUMBER

5b. GRANT NUMBER

5c. PROGRAM ELEMENT NUMBER

6. AUTHOR(S)

5d. PROJECT NUMBER
1011

5e. TASK NUMBER
0011

5f. WORK UNIT NUMBER

7. PERFORMING ORGANIZATION NAME(S) AND ADDRESS(ES)

Air Force Research Laboratory (AFMC)
AFRL/PRS
5 Pollux Drive
Edwards AFB CA 93524-7048

8. PERFORMING ORGANIZATION REPORT

9. SPONSORING / MONITORING AGENCY NAME(S) AND ADDRESS(ES)

Air Force Research Laboratory (AFMC)
AFRL/PRS
5 Pollux Drive
Edwards AFB CA 93524-7048

10. SPONSOR/MONITOR'S ACRONYM(S)

11. SPONSOR/MONITOR'S NUMBER(S)

1119 / 163

12. DISTRIBUTION / AVAILABILITY STATEMENT

Approved for public release; distribution unlimited.

13. SUPPLEMENTARY NOTES

14. ABSTRACT

15. SUBJECT TERMS

16. SECURITY CLASSIFICATION OF:

a. REPORT	b. ABSTRACT	c. THIS PAGE	17. LIMITATION OF ABSTRACT	18. NUMBER OF PAGES	19a. NAME OF RESPONSIBLE PERSON / 19b. TELEPHONE NUMBER *(include area code)*
Unclassified	Unclassified	Unclassified	A		Leilani Richardson (661) 275-5015

Standard Form 298 (Rev. 8-98)
Prescribed by ANSI Std. 239.18

7 Separate items enclosed

10110011

MEMORANDUM FOR PRS (In-House/Contractor Publication)

FROM: PROI (STINFO) 12 June 2002

SUBJECT: Authorization for Release of Technical Information, Control Number: **AFRL-PR-ED-TP-2002-139**
Greg Spanjers (PRSS) et al., "Electromagnetic Effects in the Near Field Plume Exhaust of a Micro-Pulsed Plasma Thruster"

AIAA Journal of Propulsion and Power **(Statement A)**
(Deadline = 30 June 2002)

1. This request has been reviewed by the Foreign Disclosure Office for: a.) appropriateness of distribution statement, b.) military/national critical technology, c.) export controls or distribution restrictions, d.) appropriateness for release to a foreign nation, and e.) technical sensitivity and/or economic sensitivity.
Comments:____

Signature ______________________ Date ______________

2. This request has been reviewed by the Public Affairs Office for: a.) appropriateness for public release and/or b) possible higher headquarters review.
Comments: ____

Signature ______________________ Date ______________

3. This request has been reviewed by the STINFO for: a.) changes if approved as amended, b) appropriateness of references, if applicable; and c.) format and completion of meeting clearance form if required
Comments:____

Signature ______________________ Date ______________

4. This request has been reviewed by PR for: a.) technical accuracy, b.) appropriateness for audience, c.) appropriateness of distribution statement, d.) technical sensitivity and economic sensitivity, e.) military/ national critical technology, and f.) data rights and patentability
Comments:____

APPROVED/APPROVED AS AMENDED/DISAPPROVED

____
PHILIP A. KESSEL Date
Technical Advisor
Space and Missile Propulsion Division

20021119 163

Submitted to ***Journal of Propulsion and Power***

Electromagnetic Effects in the Near Field Plume Exhaust of a micro-Pulsed Plasma Thruster

Michael Keidar and Iain D. Boyd

University of Michigan, Ann Arbor, MI 48109

Erik Antonsen*, and Gregory G. Spanjers

Air Force Research Laboratory, Propulsion Directorate, Electric Propulsion Laboratory
Edwards AFB CA 93524
** University of Illinois Urbana-Champaign*

Abstract

In this work we present a model of the near field plasma plume of a Pulsed Plasma Thruster (PPT). As a working example we consider a micro-PPT developed at the Air Force Research Laboratory. This is a miniaturized design of the axisymmetric PPT with a thrust in the 10 μN range that utilizes Teflon™™ as a propellant. The plasma plume is simulated using a hybrid fluid-PIC-DSMC approach. The plasma plume model is combined with Teflon™ ablation and plasma generation models that provide boundary conditions for the plume. This approach provides a consistent description of the plasma flow from the surface into the near plume. The magnetic field diffusion into the plume region is also considered and plasma acceleration by the electromagnetic mechanism is studied. Teflon™ ablation and plasma generation analyses show that the Teflon™ surface temperature and plasma parameters are strongly non-uniform in the radial direction. The plasma density near the propellant surface peaks at about 10^{24} m^{-3} in the middle of the propellant face while the electron temperature peaks at about 4 eV near the electrodes. The plume simulation shows that a dense plasma focus is developed at a few millimeters from the thruster exit plane at the axis. This plasma focus exists during the entire pulse, but the plasma density in the focus decreases from about 2×10^{22} m^{-3} at the beginning of the pulse down to 0.3×10^{22} m^{-3} at 5 μs. The velocity phase is centered at about 20 km/s in the axial direction. At later stages of the pulse there are two ion populations with positive and negative radial velocity. Electron densities predicted by the plume model are compared with near field measurements using a Herriot Cell technique and very good agreement is obtained.

Nomenclature

Q_j - Joule heat

Q_r - radiation heat

Q_F - heat due to the particle convection

N_e - electron density

T_e – electron temperature

V_1 - velocity at the Knudsen layer edge

Γ - ablation rate, [kg/m^{2}s]

N_1, N_2 – densities

m – heavy particle mass

T_1, T_2 - temperatures

C_s - sound speed

j – current density

B – magnetic field

E - electric field

m_e – electron mass

V_e – electron velocity

ν_{ei} – electron-ion collision frequency

σ – plasma (Spitzer) conductivity

μ – permittivity

$\omega\tau$ - Hall parameter

1. Introduction

The pulsed plasma thruster (PPT) was among the first of various electrical propulsion concepts accepted for space flight mainly due to its simplicity and hence high reliability[1]. However, the PPT has an efficiency that is generally low[2] at about 10% leaving open the opportunity for considerable improvement[3]. Currently, PPT's are considered as an attractive propulsion option for stationkeeping and drag makeup purposes on mass and power-limited satellites[4,5]. Guaranteeing successful operation of spacecraft using a PPT requires a complete assessment of the spacecraft integration effects. The PPT plume contains various ion and neutral species due to propellant decomposition and possible electrode erosion. Some attempts of PPT plume modeling using particle simulations were performed recently[6,7,8]. In Refs. 7 and 8 we have considered the plume flowfield exhaust from the recently developed electrothermal PPT (so-called PPT-4) and therefore electromagnetic effects in the plume were neglected. Different variations of electromagnetic PPTs are also candidates for various missions[9]. Recently, a micro-PPT has being designed at the Air Force Research Laboratory (AFRL) for delivery of very small impulse bit[10]. This is a simplified miniaturized version of a conventional PPT designed to provide attitude control and stationkeeping for microsatellites. We will use the AFRL micro-PPT as a working example for several reasons. Firstly, electromagnetic ($j\times B$) acceleration is the primary mechanism in this thruster; and secondly, there is no internal flow in this device and therefore the near-field plasma plume is an essential part of the thrust generation process. Therefore careful modeling of the acceleration is needed to understand the characteristics of the device as a whole in addition to being a pre-cursor to accurate estimation of contamination issues. Since in this device there is no separation between the main plasma acceleration region and the plume expansion, both regions must be simulated in one model. Because the plasma acceleration is external, the plasma is sufficiently rarefied so that an Magneto hydrodynamic (MHD) code such as MACH2 (Ref. 11) cannot be used in end-to-end simulation.

An accurate model of the PPT plume relies on the boundary and initial conditions. These conditions can be formulated by consideration of the Teflon™ ablation process. The Teflon™ ablation computation is based on a recently developed kinetic ablation model[12,13]. In this model, the detailed physics of the Teflon™ evaporation is studied by consideration of the distribution function of the particles in the kinetic layer adjacent to the surface.

Another important effect related to the plasma plume exhaust from an electromagnetic PPT is the magnetic field diffusion into the near plume. Previously, we have modeled the effect of the magnetic field on the near-field plume for Hall thrusters[14] under steady state conditions. It was found that the magnitude of the magnetic field at the thruster exit has an important effect on the plasma potential distribution in the plume. In the present research, it is proposed to include the electromagnetic effects on the near field plume of unsteady plasma flow. The computational domain is shown in Fig. 1. The model is based on a hybrid approach involving a direct simulation Monte-Carlo (DSMC) description of neutrals, a Particle-In-Cell (PIC) model for ions, and a fluid description of the electrons. In these methods, the potential distribution is usually calculated by reducing the electron momentum equation to the Boltzmann relation in the absence of a magnetic field. In the plasma plume domain where the magnetic field exists, i.e. the near field plume region, it is necessary to include the magnetic field effects in the electron momentum equation.

2. The model of the plasma layer

The model presented here describes the plasma layer near the Teflon™ surface as shown in Fig. 2. The model of the plasma layer includes Joule heating of the plasma, heat transfer to the Teflon™, and Teflon™ ablation. Mechanisms of energy transfer from the plasma column to the wall of the Teflon™ include heat transfer by particle convection and by radiation. The Teflon™ ablation computation is based on a recently developed kinetic ablation model[12] (see next section).

It is assumed that within the plasma layer all parameters vary in the radial direction, r. The energy balance equation can be written in the form:

$$\frac{3}{2}N_e\,dT_e/dt = Q_J - Q_r - Q_F \qquad (1)$$

This equation depends on the coordinate along the propellant face. For known plasma density and temperature the heat flux to the surface is calculated. The Teflon™ surface temperature is calculated from the heat transfer equation with boundary conditions that take into account vaporization heat and conductivity. The solution of this equation is considered for two limiting cases of substantial and small ablation rate very similar to that described in Ref. 8. The density at the Teflon™ surface is calculated using the equilibrium pressure for Teflon™. The plasma density in the layer is determined in the framework of the kinetic ablation model (see next section). For known pressure and electron temperature one can calculate the chemical plasma composition assuming LTE[8,15,16]. The Saha equations are supplemented by the conservation of nuclei and quasi-neutrality.

3. Ablation model

The Teflon™ ablation is modeled in the framework of the approximation[13] based on a kinetic model of the material evaporation into discharge plasmas[12]. The model couples two different layers between the surface and the plasma bulk as shown in Fig. 2: (1) a kinetic non-equilibrium layer adjusted to the surface with a thickness of about one mean free path; and (2) a collision-dominated layer with thermal and ionization non-equilibrium. The velocity at the edge of the kinetic layer, V_1, can be determined from the coupling solution of the hydrodynamic layer and the quasi-neutral plasma. For known velocity and density at this interface, it is possible to calculate

the ablation rate. In the hydrodynamic layer the relation between the velocities, temperatures and densities at the boundaries 1 and 2 as well as the ablation rate are formulated according to Ref. 13 in the form:

$$\Gamma = mV_1N_1 = N_1[(2kT_1/m)\cdot(T_2N_2/2T_1 - N_1/2)/(N_1 - N_1^2/N_2)]^{0.5} \qquad (2)$$

The system of equations is closed if the equilibrium vapor pressure can be specified that determines parameters (N_o and T_o) at the Teflon™ surface. The solution of the Knudsen layer problem relates parameters at the boundary 1 to the parameters at the boundary 0 (Ref. 12). The full self-consistent solution of this problem can be obtained when the ablation is coupled with the plasma plume expansion. In the present work in order to simplify the problem, we will assume that the plasma accelerates up to the sound speed near the boundary 2. This assumption can be justified by the fact that due to significant electrodynamic acceleration in this type of PPT, the plasma density will quickly decrease, therefore providing solution of the ablation problem close to that for ablation into vacuum. In this case the plasma density at the edge of the kinetic layer will be equal to $0.34\cdot N_o$ and the temperature is $0.7\cdot T_o$. The flux returned to the surface is equal to 16% of the ablated flux (Ref. 12).

4. Plasma plume electrodynamics

The general approach for the plume model is based on a hybrid fluid-particle approach that was used previously (Ref. 7). In this model, the neutrals and ions are modeled as particles while electrons are treated as a fluid. Elastic (momentum transfer) and non-elastic (charge exchange) collisions are included in the model. The grids employed in this computation are also similar to those used previously (Ref.7). The particle collisions are calculated using the DSMC method.[17]

Momentum exchange cross sections use the model of Dalgarno *et al.*[18], while charge exchange processes use the cross sections proposed by Sakabe and Izawa.[19] Acceleration of the charged particles is computed using the PIC method.[20] The plasma velocity distribution depends upon the magnetic field distribution and ion dynamics is calculated as follows:

$$d\mathbf{V}/dr = -C_s^2\nabla \ln(N) + \mathbf{j}x\mathbf{B}/mN \quad (3)$$

The electron dynamics is very important in the plasma plume. Previously our model was based on the assumption that electrons rapidly reach the equilibrium distribution and in the absence of the magnetic field can be described according to the Boltzmann distribution. While this was a satisfactory assumption in the case of an electrothermal thruster plume this is not suitable for the near field of an electromagnetic thruster. In the presence of a strong magnetic field, the electron density distribution deviates from that according to Boltzmann[21]. In the case of a magnetic field the electron momentum equation reads (neglecting electron inertia):

$$0 = -e^2N_e(\mathbf{E}+\mathbf{V}_e\times\mathbf{B}) - e\nabla P_e - \nu_{ei}m_e\mathbf{j} \quad (4)$$

We have assumed quasi-neutrality therefore $N_e = N_i = N$. The electric and magnetic field distributions in the plume are calculated from the set of Maxwell equations. We further assume that the magnetic field has only an azimuthal component and also neglect the displacement current. The combination of the Maxwell equations and electron momentum conservation gives the following equation for the magnetic field:

$$\partial\mathbf{B}/\partial t = 1/(\sigma\mu)\nabla^2\mathbf{B} - \nabla\times(\mathbf{j}\times\mathbf{B}/(eN)) + \nabla\times(\mathbf{V}\times\mathbf{B}) \quad (5)$$

A scaling analysis shows that the various terms on the right hand side of Eq. 5 may have importance in different regions of the plasma plume and therefore a general end-to-end plasma plume analysis requires keeping all terms in the equation. In the case of the near plume of the micro-PPT with a characteristic scale length of about 1 cm the magnetic Reynolds number $Re_m \ll 1$ and therefore the last term can be neglected. Taking this into account in dimensionless form, Eq. 5 can be written as:

$$Re_m \partial \mathbf{B}/\partial t = \nabla^2 \mathbf{B} - (\omega\tau)\cdot\{\nabla\times(\nabla\times\mathbf{B}\times\mathbf{B})\} \quad (6)$$

where $(\omega\tau)$ is the Hall parameter that measures the Hall effect. Therefore, depending on the plasma density, the Hall effect may be important for the magnetic field evolution. One of the first calculations of the plasma flow with Hall effect were performed by Brushlinski and Morozov (see Ref. 22 and references therein). They considered isothermal flow. The plasma density becomes high at the cathode and lower at the anode. The Hall effect has a particularly noticeable influence on the magnetic field distribution. The field near the anode increases and near the cathode decreases. As a result the current is deflected to the side and grazes the anode.

Our estimations show that the Hall parameter $\omega\tau \ll 1$ if the plasma density near the Teflon™ surface $N > 10^{23}$ m^{-3}. This case is realized in the micro-PPT (see the next section) so the Hall effect is expected to be small for this particular case. Therefore all results presented below are calculated without considering Hall effect. Having the magnetic field distribution one can calculate the current density distribution from Ampere's law:

$$\mu \mathbf{j} = \nabla \mathrm{x} \mathbf{B} \quad (7)$$

The magnetic field and current distributions calculated from this model are used in PIC to evaluate the ion dynamics according to Eq. 3.

5. Boundary conditions

The boundary conditions for the magnetic field calculations are shown in Fig. 1. We assume that the current is uniform on both electrodes that allows us to estimate the current density on the cathode j_c and on the anode j_a. The magnetic field is assumed to vary as 1/r on the upstream boundary. At the lateral boundary we assume that the normal current j_n=0. The downstream boundary is considered to be far enough away that B=0 can be assumed. Along the centerline the magnetic field is zero.

The boundary conditions for the plume are generated through solution of the Teflon™ ablation problem as will be presented in the Results section. These involve time and radial dependent variations of the plasma (including Carbon and Flourine ions and neutrals) density and electron temperature.

The results are presented for a 3.6 mm (0.141") diameter micro-PPT, which has a 0.9 mm diameter central electrode, 3.1 mm propellant diameter and 0.24 mm anode wall (Ref. 10). In these simulations, the experimental current waveform is used, that is described in a first approximation as an underdamped LRC circuit current:

$I(t) = I_p \cdot \sin(\alpha t)\exp(-\beta t)$ ....(8)

where $I_p = \sqrt{\frac{2E}{L}}$; $\alpha = \sqrt{\frac{1}{LC}}$; $\beta = \frac{R}{2L}$; L is the effective inductance in the circuit, C is the capacitance, R is the total circuit resistance, and E is the pulse energy. Results presented below correspond to E=2.25 J and C=0.5 μF. The best fit with the experimental waveform (frequency) corresponds to $\alpha = 4.7 \cdot 10^7$ rad/s and circuit inductance L=90 nH.

6. Results

The plasma density and electron temperature distribution are also shown in Figs. 3a-3b. The plasma density peaks at about 10^{24} m^{-3} midway between the electrodes. The electron temperature is strongly non-uniform radially with peaks near the electrodes of about 4.5 eV as shown in Fig. 3b. The reason for higher electron temperature near the electrodes is due to current spreading in the space between the electrodes and current focusing near the electrodes (see below results on current distribution).

The spatial and temporal variation of the Teflon™ surface temperature is shown in Fig. 3c. The Teflon™ temperature sharply increases during the first 2 μs of the pulse and peaks at about 960 K. One can see that the temperature is generally non-uniform in the radial direction and has a minimum at radial distances of 1.1-1.3 mm. Since the Teflon™ ablation is approximately exponentially proportional to the surface temperature, the model predicts a lower rate of ablation in the areas where the surface temperature has a minimum. Taking this into account, the effect of the temperature distribution may be related to the preferential charring of the Teflon™ surface observed experimentally [Ref. 10]. As was mentioned earlier, the ablation rate is also non-uniform radially. This effect is shown in Fig. 3d. One can see that the ablation rate peaks near the electrodes at about 60 kg/m^2s, while in the middle of the propellant face it is about 30-40 kg/m^2s. The calculated total ablated mass per pulse is about 1.4 μg.

A region of magnetic field diffusion in the near field outside the micro-PPT is shown in Fig. 4a. The magnetic field drops by an order of magnitude at about 1.5 mm that is equal to the thruster radius. This is also the region where most of the current is concentrated as shown in Fig. 4b. One can see that the current density is high near the central electrode and near the outer electrode. This is a reason for the increasing Teflon™ surface temperature and electron temperature in these regions. According to the model presented in Sec. 4 the electromagnetic acceleration of the plasma is also expected to occur in this region.

Figure 5 shows evolution of the Carbon ion (C+) component of the plasma plume during the main part of the pulse. One can see that a dense plasma focus is developed at a few millimeters from the thruster exit plane. This plasma focus exists during the entire pulse as shown in Fig. 5, but the plasma density in the focus decreases from about 2×10^{22} m^{-3} at the beginning of the pulse down to 0.3×10^{22} m^{-3} at 5 μs. At the beginning (first 2 μs) the C+ density mainly develops a gradient in the radial direction that is a result of high directed velocity in the axial direction. Later, during the pulse, the axial density gradient becomes comparable to the radial one.

The Flourine ions (F+), due to their larger mass, have different dynamics as shown in Fig.6. They have smaller acceleration in the axial direction even at the beginning of the pulse and therefore both axial and radial density gradients are developed. The F+ density in the plume and in the plasma focus is larger than that of C+, because originally Teflon™ has composition C_2F_4 with F density twice larger than that of C. Additionally F ions experience less acceleration in the plume because of their higher mass that also contributes to their relative density increase.

The micro-PPT is essentially an electromagnetic accelerator as shown in the velocity phase plots (Figs. 7,8). The phase plot of the Carbon ions at 1 μs is centered at 20 km/s in the axial direction. Ions experience also radial expansion in both directions due to the magnetic field structure and the temperature expansion. The radial velocity in the negative direction is related to the focus formation along the axis, as shown in Figs. 5, 6. The Flourine ions generally have both smaller axial and radial velocities due to their higher mass. At a later stage of the pulse (see Fig. 8) clearly there are two ion populations with positive and negative radial velocities. This is due to the annular plasma injection corresponding to the thruster geometry (see Figs. 1,2).

During the entire pulse there is a population of ions having a negative axial velocity with the magnitude up to about 10 km/s (see Figs. 7,8). This population creates the backflow contamination that occurs mainly onto the thruster itself. The Carbon ions have a larger negative velocity due to their higher mobility that results in their domination in the backflux. This backflux may be mainly responsible for charring phenomena observed in this thruster (see Ref. 10).

7. Comparison with experiment

In this section we present measured and predicted electron density distributions in the near field plume for one micro-PPT design. These data will be compared in order to assess our plume and device model.

An experimental basis for comparison is provided using a Herriott Cell interferometer. Electron density measurements are taken on a 6.35 mm (1/4") diameter micro-PPT at AFRL. The interferometer uses a single laser wavelength and quadrature heterodyne technique described by Spanjers *et al.*[23] Addition of a Herriott Cell acts to confine a large number of laser passes into an area suitable for maximum exposure to the MicroPPT plume. This is achieved by focusing the

laser between the two concave mirrors of the cell. The technique is used to increase signal-to-noise ratio for diffuse plasmas by increasing laser exposure to the plasma over a characteristic path length.[24] Thirteen laser reflections in the Herriott Cell were focused to two points, separated by 3 mm. For data shown here, these points formed a plane parallel to the fuel face and 5 mm distant. More details about the Herriott Cell technique can be found elsewhere.[24]

Figure 9 shows the experimental data co-plotted with model predictions. Plasma density peaks at about 3×10^{16} cm^{-3} and decreases by several orders of magnitude towards the pulse end. The experimental data was taken at a discharge energy of 6.6 J from a 0.417 μF capacitor. Experimental waveforms of the current were obtained using a self-integrating Rogowski coil. Peak density reaches $23\pm6\cdot10^{15}$ cm^{-3} with uncertainty due to shot-to-shot variations in thruster firing. One can see that the model correctly predicts both the plasma density level and temporal behavior during the entire pulse.

7. Concluding remarks

In this paper, a self-consistent description of an electromagnetic pulsed plasma thruster from plasma generation into the near plume was presented. A micro-PPT developed at AFRL was considered as a working example. In this device, no separation exists between the main plasma acceleration region, which usually occurs in an internal flow, and the external plasma plume field. Therefore, a single end-to-end model is necessary for accurate simulations. A kinetic Teflon™ ablation model was incorporated in order to provide the boundary conditions for the plasma plume.

The phenomena in the plasma plume related to the electromagnetic effects were studied. The plume simulation showed that a dense plasma focus developed at a few millimeters from the thruster exit plane at the axis. This plasma focus exists during the entire pulse, but the plasma density in the focus decreases from about 2×10^{22} m^{-3} at the beginning of the pulse down 0.3×10^{22} m^{-3} at 5 μs. The velocity phase is centered at about 30 km/s in the axial direction demonstrating that the micro-PPT is essentially an electromagnetic accelerator. At a later stage of the pulse there are two ion populations with positive and negative radial velocity. It is predicted that there is a population of ions having a negative axial velocity magnitude up to about 10 km/s. This population creates the backflow contamination that flows mainly onto the thruster itself. The Carbon ions have a larger negative velocity due to their higher mobility that results in their domination in the backflux. It is believed that this backflux is responsible for the charring phenomena observed in this thruster.

Predicted electron density in the near-field plume was directly compared with experimental data and very good agreement was obtained.

Acknowledgements

The first authors gratefully acknowledge financial support by the Air Force Office of Scientific Research through grant F49620-99-1-0040.

Figure Captions

Figure 1. Schematic diagram of micro-PPT plume and boundary conditions

Figure 2. Schematic of the near Teflon™ plasma layer

Figure 3. Spatio-temporal distribution: (a) Teflon™ surface temperature, (b) plasma density, (c) electron temperature, and (d) ablation rate.

Figure 4. (a) Magnetic field distribution and (b) current line vectors in the near field of the micro-PPT.

Figure 5. Evolution of the Carbon ion density during the pulse

Figure 6. Evolution of the Flourine ion density during the pulse

Figure 7. Ion velocity phase. Early stage of the pulse

Figure 8. Ion velocity phase. Late stage of the pulse

Figure 9. Comparison of predicted and measured electron density time variation at 5 mm from the propellant face at the axis in the case of the 6.35 mm diameter micro-PPT firing at 6.6 J.

REFERENCES

[1] R. L. Burton and P. J. Turchi, "Pulsed plasma thruster", Journal of Propulsion and Power, Vol.14, No. 5, 1998, pp. 716-735.

[2] R.J. Vondra and K.I. Thomassen, "Flight qualified pulsed plasma thruster for satellite control", *Journal of Spacecraft and Rockets*, Vol. 11, No. 9, 1974, pp. 613-617.

[3] P. J. Turchi, Directions for improving PPT performance, *Proceeding of the 25th International Electric Propulsion Conference*, vol. 1, Worthington, OH, 1998, pp. 251-258.

[4] E. Y. Choueiri, "System optimization of ablative pulsed plasma thruster for stationkeeping", *Journal of Spacecraft and Rockets*, Vol. 33, No. 1, 1996, pp. 96-100.

[5] R. A. Spores, R. B. Cohen and M. Birkan, "The USAF Electric propulsion program", *Proceeding of the 25th International Electric Propulsion Conference*, vol. 1, Worthington, OH, 1997, p.1.

[6] N. A. Gatsonis and X. Yin, Axisymmetric DSMC/PIC simulation of quasineutral partially ionized jets, AIAA paper 97-2535, July 1997.

[7] I. D. Boyd, M. Keidar, and W. McKeon, Modeling of a pulsed plasma thruster from plasma generation to plume far field, *Journal of Spacecraft and Rockets, Vol. 37, No. 3, 2000, pp. 399-407*

[8] M. Keidar and I.D. Boyd, "Device and plume model of an electrothermal pulsed plasma thruster", Paper AIAA-2000-3430, July 2000.

[9] W.A. Hoskins and R.J. Cassady, " Applications for Pulsed Plasma Thrusters and the Development of Small PPTs for Microspacecraft", AIAA-2000-3434, July 2000.

[10] F. Gulczinski III, M. Dulligan, J. Lakes and G. Spanjers, "Micropropulsion research at AFRL", Paper AIAA-2000-3255, July 2000

[11] P.G. Mikellides and P. J. Turchi, "Modeling of late-time ablation in Teflon™ pulsed plasma thruster", AIAA Paper 96-2733, July 1996.

[12] M. Keidar, J. Fan, I.D. Boyd and I.I. Beilis, "Vaporization of heated materials into discharge plasmas", Journal of Applied Physics, 89, 2001, pp. 3095-3098.

[13] M. Keidar, I.D. Boyd and I.I. Beilis, "On the model of Teflon™ ablation in an ablation-controlled discharge", Journal of Physics D: Applied Physics, 34, June, 2001, pp. 1675-1677.

[14] M. Keidar and I.D. Boyd, "Effect of a magnetic field on the plasma plume from Hall thruster", Journal of Applied Physics, 86, 1999, pp. 4786-4791.

[15] P. Kovatya, Thermodynamic and transport properties of ablated vapors of PTFE, alumina, perspex and PVC in the temperature range 5000-30000 K, IEEE Transaction on Plasma Science, 12, 1984 pp. 38-42.

[16] C.S. Schmahl and P.J. Turchi, Development of equation-of-state and transport properties for molecular plasmas in pulsed plasma thrusters. Part I: A two-temperature equation of state for Teflon™, Proc. Inter. Electr. Propul. Conf. Pp. 781-788, 1997.

[17] G.A. Bird, "*Molecular gas dynamics and the direct simulation of gas flows*" (Clarendon Press, Oxford, 1994).

[18] A. Dalgarno, M.R.C. McDowell and A. Williams, The modilities of ions in unlike gases, Proc. Of Royal Soc. Of London, Vol. 250, April 1958, pp. 411-425.

[19] S. Sakabe and Y. Izawa, Simple formula for the cross sections of resonant charge transfer between atoms and their ions at low impact velocity, Physical Rev. A: General Physics, v. 45, No. 3, 1992, pp. 2086-2089.

[20] C.K. Birdsall and A.B. Langdon, Plasma Physics via Computer Simulation, Adam Hilger Press, 1991.

[21] I.I. Beilis, M. Keidar and S. Goldsmith, "Plasma-wall transition: The influence of the electron to ion current ratio on the magnetic presheath structure", Physics of Plasmas, 4, 1997, pp. 3461-3468.

[22] K.V. Brushlinski and A.I. Morozov, "Calculation of two-dimensional plasma flows in channels", in Rev. Plasma Physics, Ed. M.A. Leontovich, Volume 8, 1980, Consultants Bureau, New York.

[23] G.G. Spanjers, K.A. McFall, F. Gulczinski III, R.A. Spores, "Investigation of Propellant Inefficiencies in a Pulsed Plasma Thruster, AIAA Paper 96-2723, July 1996

[24] E.L. Antonsen, Herriott Cell Interferometry for Pulsed Plasma Density Measurements, MS Thesis, University of Illinois at Urbana-Champaign, 2001

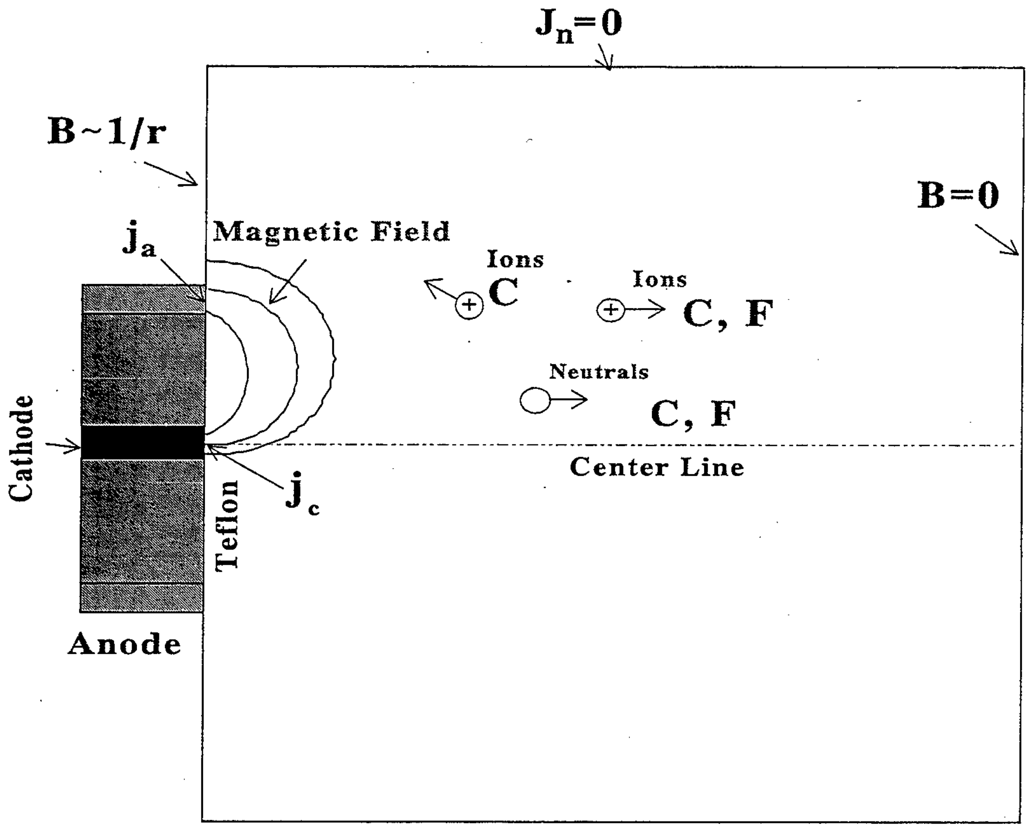

Figure 1. Keidar *et al.* "Electromagnetic effects…"

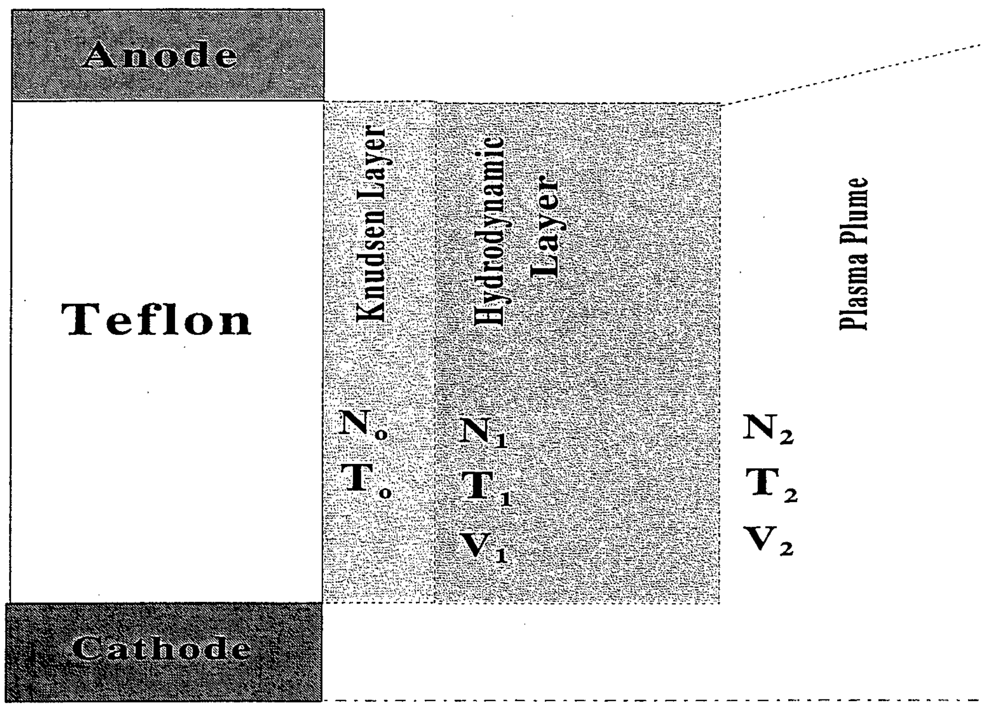

Figure 2. Keidar *et al.* "Electromagnetic effects…"

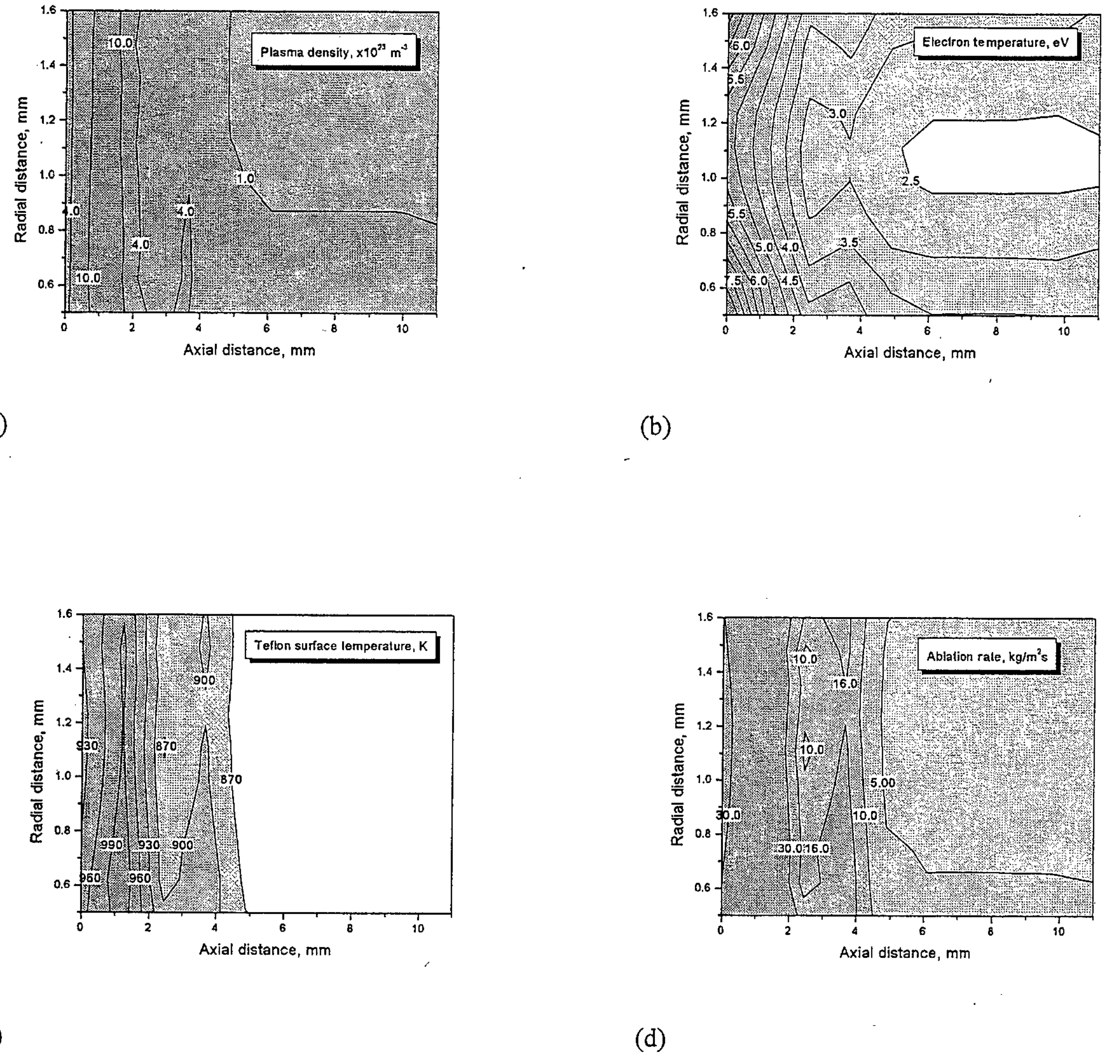

Figure 3. Keidar *et al.* "Electromagnetic effects…"

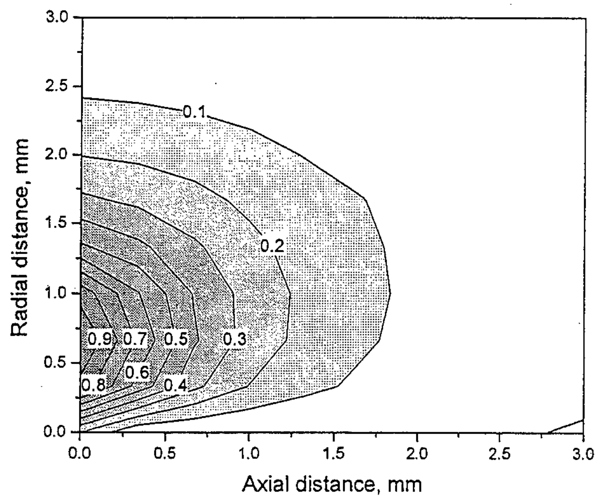

(a)

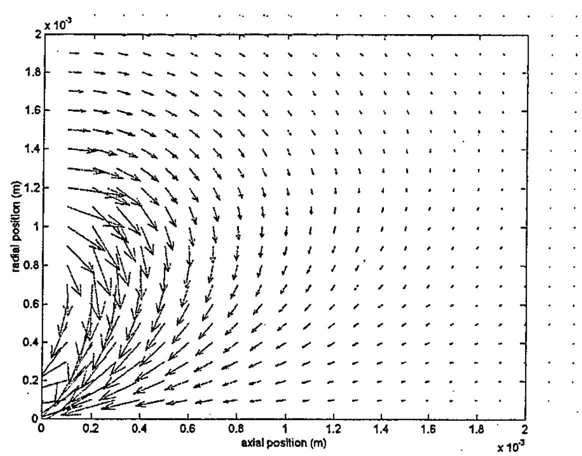

(b)

Figure 4. Keidar *et al.* "Electromagnetic effects…"

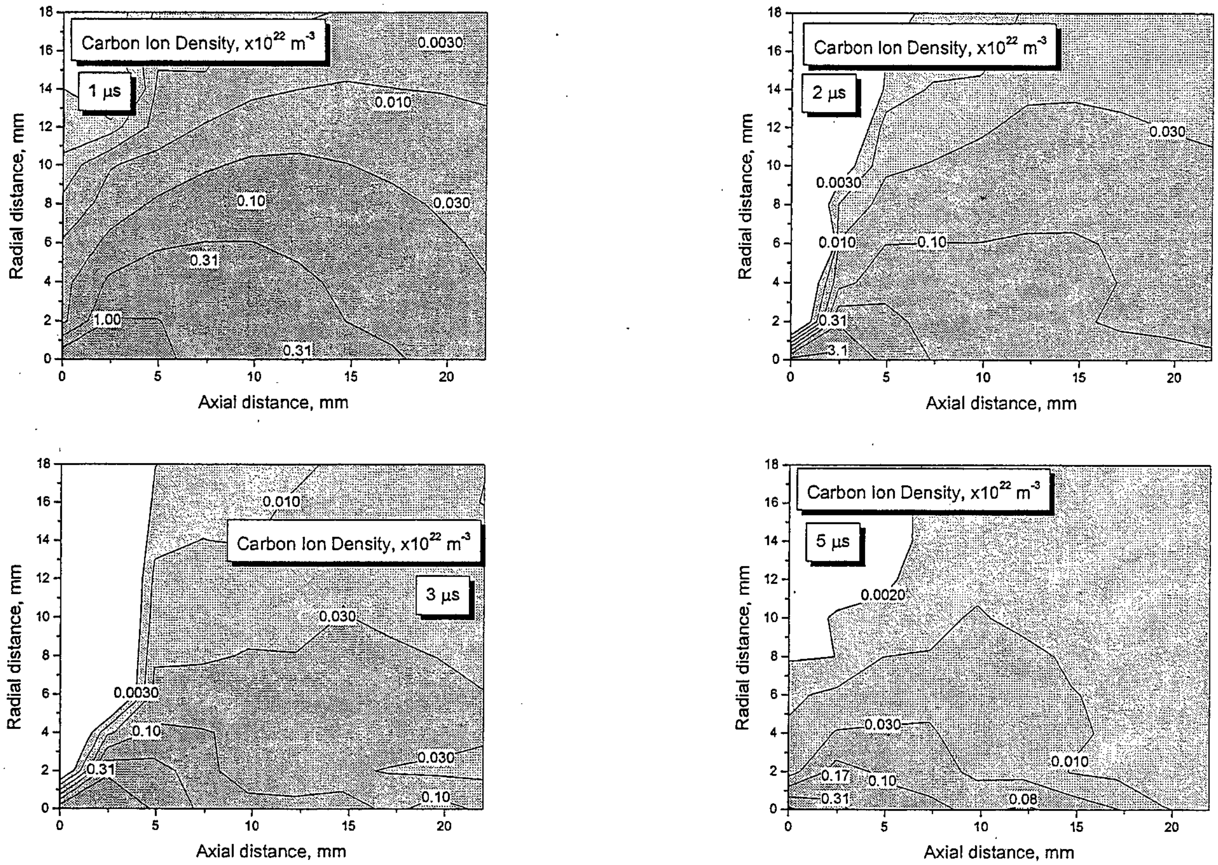

Figure 5. Keidar *et al.* "Electromagnetic effects…"

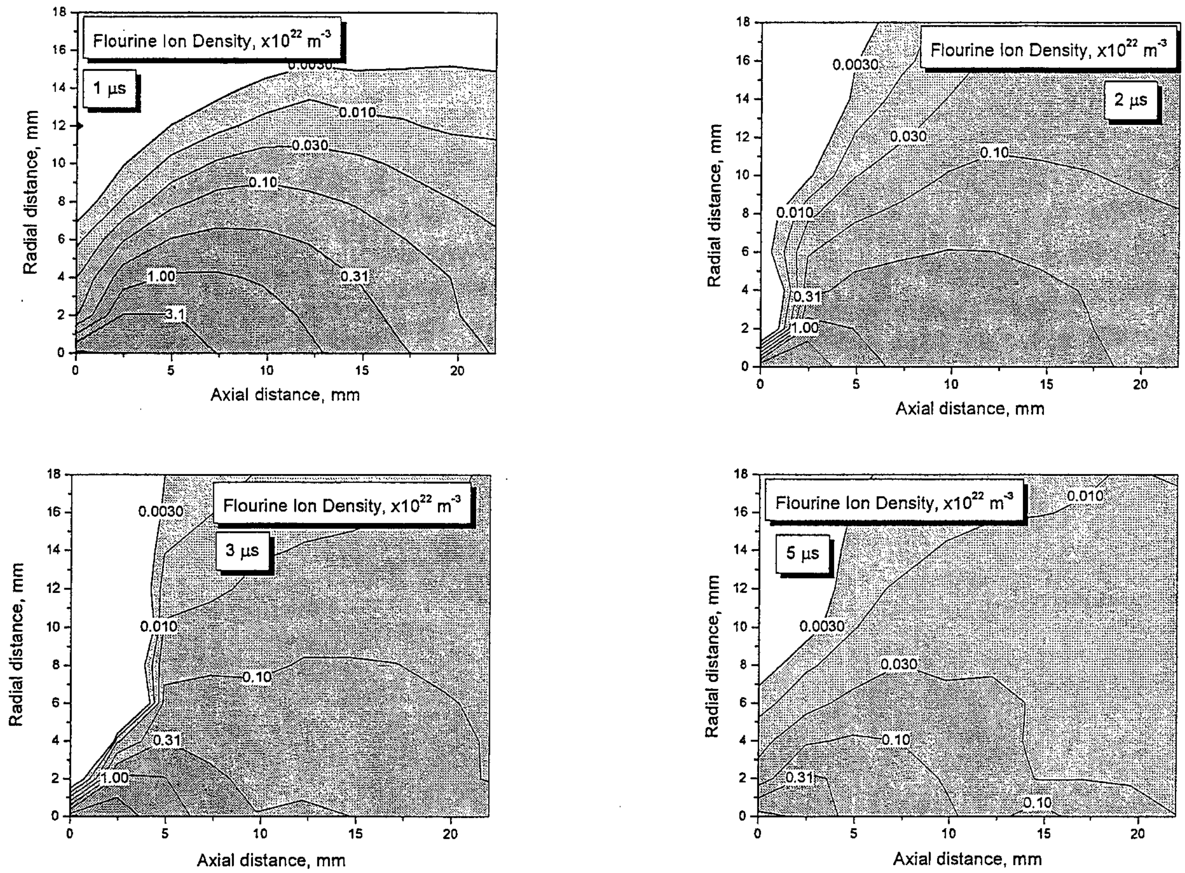

Figure 6. Keidar *et al.* "Electromagnetic effects…"

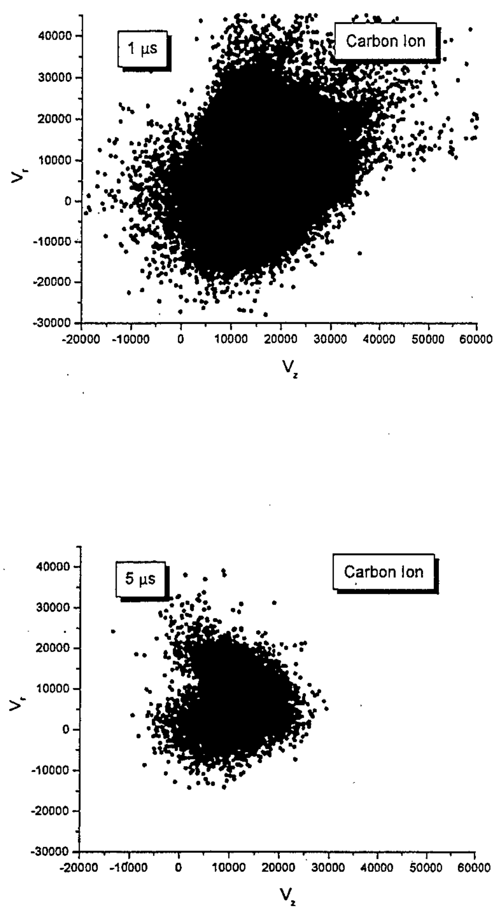

Figure 7. Keidar *et al.* "Electromagnetic effects…"

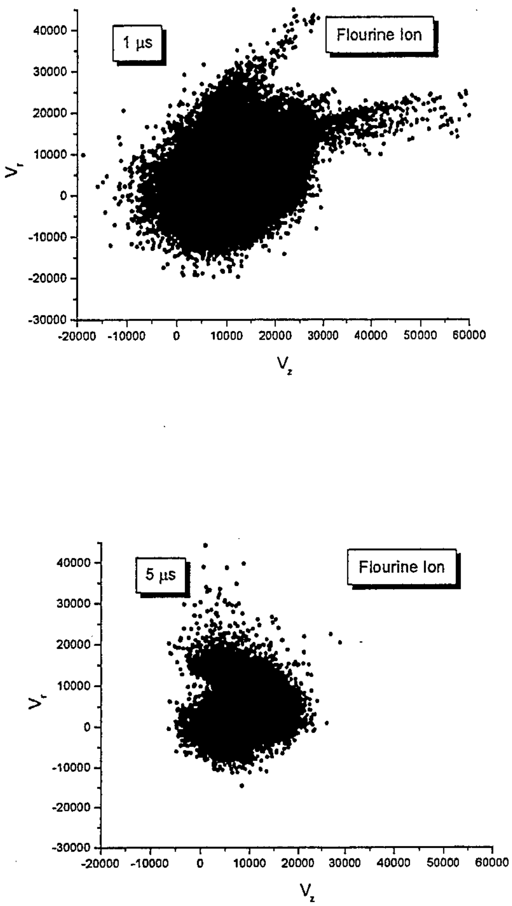

Figure 8. Keidar *et al.* "Electromagnetic effects…"

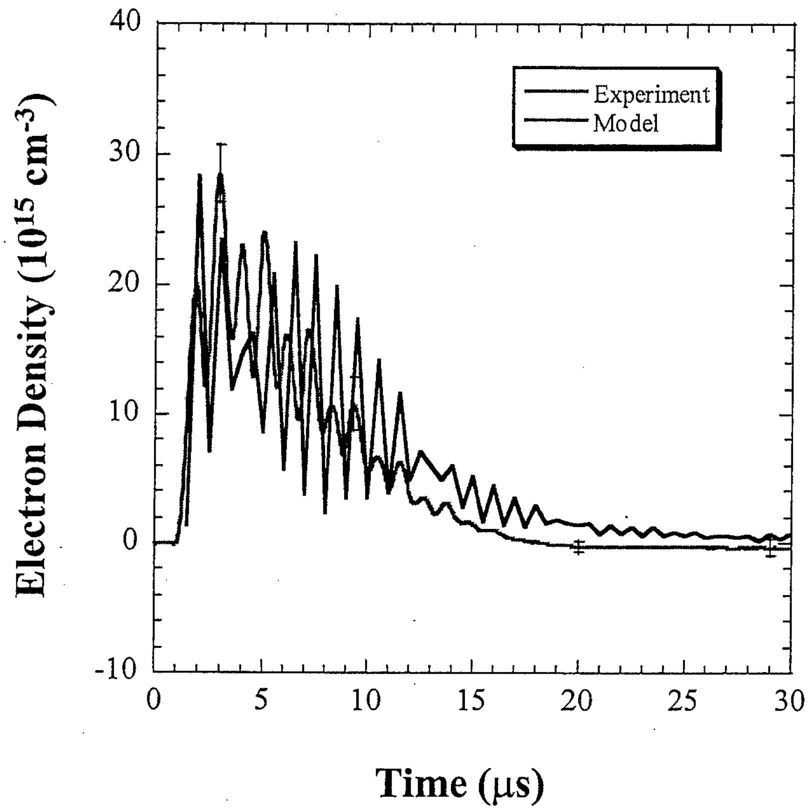

Figure 9. Keidar *et al.* "Electromagnetic effects…"